LIPID MAPPING OF THE RAT BRAIN FOR MODELS OF DISEASE

[1]Martínez-Gardeazabal J, [1]González de San Román E, [1]Moreno M, [1]Llorente-Ovejero A, [1]Manuel I, [1]Rodriguez-Puertas R

[1]*Department of Pharmacology, Faculty of Medicine and Nursing. University of the Basque Country (UPV/EHU), Bº Sarriena s/n, 48940 Leioa, Spain*

*Corresponding author:

Rafael Rodríguez-Puertas

Department of Pharmacology. Faculty of Medicine and Nursing.

University of the Basque Country. E-48940, Leioa, Vizcaya. Spain.

E-mail: rafael.rodriguez@ehu.eus

Tel.: +34-94-6012739; fax: +34-94-6013220.

1

[1] **Abbreviations**

2-AG	2-araquinodonoylglycerol
AChE	Acetylcholinesterase
aCSF	Artificial Cerebrospinal Fluid
AD	Alzheimer's Disease
AEA	Anandamide
CNS	Central Nervous System
CPA	Cyclic phosphatidic acid
GlcCer	Glucosylceramide
GSL	Glycosphingolipid
LacCer	Lactosylceramide
LPA	Lysophosphatidic acid
LPC	Lysophosphatidylcholine
LPI	Lysophosphatidylinositol
MALDI –IMS	Matrix-Assisted Laser Desorption / Ionization Imaging Mass Spectrometry
MBT	2-mercaptobenzothiazole
NBM	Nucleus Basalis Magnocellularis
p75NTR	Low-affinity nerve growth factor
PA	Phosphatidic acid
PC	Phosphatidylcholines
PE	Phosphatidylethanolamine
PG	Phosphatidylglycerol
PI	Phosphatidylinositol
PL	Phospholipid
PLA2	Phospholipase A2
PS	Phosphatidylserine
S1P	Sphingosine 1-phosphate
SAP	192IgG-saporin
SM	Sphingomyelin
ST	Sulfatide

Abstract

Lipids not only constitute the primary component of cellular membranes and contribute to metabolism but also serve as intracellular signaling molecules and bind to specific membrane receptors to control cell proliferation, growth and convey neuroprotection. Over the last several decades, the development of new analytical techniques, such as imaging mass spectrometry (IMS), has contributed to our understanding of their involvement in physiological and pathological conditions. IMS allows researchers to obtain a wide range of information about the spatial distribution and abundance of the different lipid molecules that is crucial to understand brain functions.

The primary aim of this study was to map the spatial distribution of different lipid species in the rat central nervous system (CNS) using IMS to find a possible relationship between anatomical localization and physiology. The data obtained were subsequently applied to a model of neurological disease, the 192IgG-saporin lesion model of memory impairment.

The results were obtained using a LTQ-Orbitrap XL mass spectrometer in positive and negative ionization modes and analyzed by ImageQuest and MSIReader software.

A total of 176 different molecules were recorded based on the specific localization of their intensities. However, only 34 lipid species in negative mode and 51 in positive were assigned to known molecules with an error of 5 ppm. These molecules were grouped by different lipid families, resulting in: Phosphatidylcholines (PC): PC (34: 1) + K^+ and PC (32: 0) + K^+ distributed primarily in grey matter, and PC (36: 1) + K^+ and PC (38: 1) + Na^+ distributed in white matter. Phosphatidic acid (PA): PA (38: 3) + K^+ in white matter, and PA (38: 5) + K^+ in grey matter and brain ventricles. Phosphoinositol (PI): PI (18: 0/20: 4) – H^+ in grey matter, and PI (O-30: 1) or PI (P-30: 0) - H^+ in white matter. Phosphatidylserines (PS): PS (34: 1) - H^+ in grey matter, and PS (38: 1) - H^+ in white matter. Sphingomyelin (SM) SM (d18: 1/16: 0) - H^+ in ventricles and SM (d18: 1/18: 0) - H^+ in grey matter. Sulfatides (ST): ST (d18: 1/24: 1) – H^+ in white matter. The specific distribution of different lipids supports their involvement not only in structural and metabolic functions but also as intracellular effectors or specific receptor ligands and/or precursors. Moreover, the specific localization in the CNS described here will enable us to analyze lipid distribution to identify their physiological conditions in rat models of neurodegenerative pathologies, such as Alzheimer's disease.

1. Introduction

The major components of plasma membranes are lipids. These molecules have a wide range of functions including cellular structure, metabolism and signaling molecules [1]. Regarding this last feature, there is a group of lipid species that are distinguished by their involvement in neurotransmission, primarily acting as neuromodulators of other systems. These specific lipids reach their highest degree of specialization and diversity in the central nervous system (CNS), and could be called neurolipids in the same way that neuronal-specific proteins are called neuropeptides. Some of these lipids that act as signaling molecules originate from phospholipid (PL) precursors present in the plasma membrane and are synthesized on demand. Representative systems are the endocannabinoid, with 2-araquinodonoylglycerol (2-AG) and anandamide (AEA), and the sphingolipid system, with the sphingosine 1-phosphate (S1P). Other neurolipid mediators, such as the lysophosphatidic acid (LPA), can originate from different locations.

The functions of specific neurolipids in the CNS are complex and diverse, and depend on anatomical distribution. LPA is involved in neurogenesis during embryo development and differentiation [2,3], in roles that include myelination and cell migration [4-6]. The sphingolipid S1P also regulates cell migration and cellular growth [7,8], and it also functions in inhibiting apoptotic processes [9,10] and intracellular Ca^{2+} signaling [11]. Moreover, therapeutic potential for these molecules is emerging based on neuroprotective effects that have been demonstrated for the endocannabinoids [12,13], as well as their ability to be regulated by specific enzymes and membrane receptors in discrete areas of the brain [14].

The progress achieved in the field of lipidomics has been accompanied by the development of new techniques to detect and analyze specific lipid species. Matrix-assisted laser desorption/ionization imaging mass spectrometry (MALDI-IMS) has an advantage over conventional MS techniques because, in addition to identifying a multiplicity of lipid molecules, it offers unbiased visualization of the spatial arrangement of lipids in tissue. This feature allows researchers to infer the physiological functions of membrane lipids in the brain [15-17].

Therefore, IMS constitutes a remarkable advance in CNS lipidomic research that will certainly help us to understand the complex pathogenic mechanisms responsible for the clinical manifestations of neurodegenerative diseases, such as Alzheimer's disease (AD).

Previous studies applying mass spectrometry techniques to lipid extracts of brain or plasma samples from AD patients have identified modulations in specific lipid species

[18,19]. Animal models remain invaluable tools for research on different diseases. Together, IMS and animal models are already contributing to the development of new therapies based on targeting neurolipids and the associated enzymatic machinery to restore lipid homeostasis in specialized brain areas and vulnerable neurotransmitter systems. For AD, the vulnerability of the cholinergic system in the basal forebrain is used to mimic clinical symptoms of the disease in a rat model, which uses a 192IgG-saporin-induced lesion of P75 neurotrophin receptor-expressing neurons in the nucleus basalis magnocellularis (NBM) [20-22].

The present study describes mapping the distribution of different complex lipid molecules, particularly phospholipids, that are present in cell membranes of neurons and glia in the rat brain. We also describe modulation of this lipid profile in the rat model of cholinergic lesions used to assay therapies for AD.

2. Materials and Methods

2.1 Animals and tissue preparation

Two month old male Sprague-Dawley rats (200-250 g) were used for the study. The animals were housed under the following conditions: day:night cycle (12:12 h), 22 ºC, 65% humidity, and with food and water *ad libitum*. The experimental protocols were approved by the Local Ethics Committee for animal research of University of the Basque Country (EAEC/388/2014) according to EU directives 2010/63/EU for animal experiments.

2.2 192IgG-saporin administration

The rats used to localize lipid species in our model of memory impairment were divided into two groups. In the first group, artificial cerebrospinal fluid (aCSF) (148 mM NaCl, 2.7 mM KCl, 0.85 mM $MgCl_2.6H_2O$, 1.2 mM $CaCl_2.2H_2O$, pH 7.4 adjusted with 1 mM K_2HPO_4) was administered (1 µl/hemisphere). In the second group, the toxin 192IgG-saporin (SAP) in aCSF (135 ng/1 µl/hemisphere; 0.25 µl/min) was administered. The intraparenquimal administration was performed using stereotaxic coordinates on Bregma: AP -1.5 mm, ML ± 3 mm, AA +8 mm [23] in the nucleus basalis magnocellularis (NBM) with a Hamilton Neurosyringe®, where the toxin is recognized by cholinergic cells expressing low-affinity nerve growth factor receptor ($p75^{NTR}$). When internalized, the toxin inhibits protein synthesis, thereby producing specific death of this cell type.

2.3 Passive avoidance test

In order to assess the behavioral effects of the administration of 192IgG-saporin toxin the passive avoidance test (passive evasion box of PanLab LE870 / 872) was performed 7 days after the surgery. The apparatus is separated in two compartments by a guillotine door, one of them is the illuminated compartment, which is white, wide and opened; while the second is the dark compartment, which is black, small and closed. The passive avoidance test consists in two procedures, the acquisition procedure and retention procedure. In the first one, each animal was placed in the illuminated compartment and after 30 sec of exploration the guillotine door is opened, allowing the animal to enter in the dark compartment for 60 sec. When the animal enters in the dark compartment, the guillotine door was closed and the latency of

acquisition was measured, and so foot shock (0.4 mA/2 sec) was delivered. Those rats that did not enter the dark compartment were removed from the study. After 24h, the retention procedure was performed by placing the animal back into the illuminated compartment allowing to explore for 30 sec, after that, the guillotine door was opened and the step through latency time to enter the dark compartment was measured up to a maximum cut-off time of 300 sec.

2.4. Acetylcholinesterase staining

Histochemical procedures were used to evaluate the cholinergic system in the basal forebrain and projection areas. The procedure for the acetylcholinesterase (AChE) staining was carried out by “direct coloring” thiocoline method. This reaction was performed to stain cholinergic neuron in the NBM and cholinergic innervations. The sections were rinsed twice in 0.1 M Tris-Maleate buffer (pH 6.0) for 10 min and therefore were incubated in darkness with constant agitation in the AChE reaction buffer: 0.1 M Tris-Maleate; 5 mM sodium citrate; 3 mM $CuSO_4$; 0.1 mM iso-OMPA; 0.5 mM $K_3Fe(CN)_6$ and 2 mM acetylthiocholine iodide as reaction substrate. The cholinergic somas in NBM were stained after 30 min of incubation time. Later on, the enzymatic reaction was stopped in two consecutive washes (2x10 min) in 0.1 M Tris-maleate (pH 6.0). After that, the samples were then dehydrated in increasing concentrations of ethanol and covered with DPX as the mounting medium.

2.5. Quantification of AChE staining and statistical analyses.

To obtain the total number of cholinergic neurons (N) of NBM, stained cells were counted independently by two observers at three different stereotaxic levels (-1.08 mm, -1.56 mm and -2.04 mm AP from Bregma). So, the population of cholinergic neurons was expressed as N/mm^3. Subsequently, a linear regression analysis was made between step through latency times and cholinergic neurons density in the NBM and Pearson´s correlation coefficient was calculated. The statistical significance threshold was set at $p<0.05$.

2.6 Sample preparation for MALDI-IMS

Rat brains were quickly removed by dissection after anesthesia, then frozen and kept at -80ºC. Next, the brains were cut on a Microm HM550 cryostat (Walldorf, Germany) to obtain 20 µm sections that were mounted onto gelatin-coated slides. They were

maintained at -20 ºC until the experiment was performed. On the day of the experiment, the tissue samples were dried by a glass sublimator (ACE glass 8023, USA) at room temperature for 15 minutes prior to deposition of the matrix onto the tissue. The sublimation was performed with 300 mg of 2-mercaptobenzothiazole (MBT) in the sublimator at 100° C for 23 minutes, followed by a re-crystallization process on the bottom of a Petri plate with methanol at 38ºC for one minute [17]. This step allows for achieving higher intensities in the mass detection.

2.7 Mass spectrometer

An LTQ-Orbitrap-XL mass spectrometer (Thermo Fisher Scientific, San Jose, CA) was used. The system was equipped with a nitrogen laser of λ= 337 nm, using a repetition rate= 60 Hz and a spot size= 80 x 120 µm. Each slice was scanned in both positive ionization mode, in the range of m/z 500-1000, and negative ionization mode, in the range of m/z 400-1100. The parameters used to obtain sagittal images of the rat brain in non-treated animals were 2 micro scans/step with 10 laser shots and a raster step size of 100 µm at laser fluence of 40 µJ. The parameters used to obtain coronal images of lipid intensity in the rat model of cholinergic basal forebrain injury, were 2 micro scans/step with 10 laser shots and a raster step size of 150 µm at laser fluence of 15 µJ.

2.8 Image and spectrum analysis for MALDI-IMS

Mass spectra were obtained with ImageQuest software (Thermo Scientific, San Jose, CA), which identifies a wide variety of m/z. The intensity of each identified molecule (m/z) is calculated in a region of interest as the average intensity of every pixel. The normalization of spectra was made as a ratio of the maximum peak, which was set at 100%, and the average intensities were calculated by OriginPro 8 software. The images were extracted with MSiReader software [24].

2.9 Peak assignment and statistics

A large number of molecules were detected, with some of them sharing very similar mass. This made it difficult to accurately assign an m/z value to a specific lipid molecule. Moreover, some of the m/z values obtained was not assigned because they have not been previously assigned in the reference database used (e.g., lipid maps; www.lipidmaps.org). The number of m/z values (hundreds) that were obtained was too

high for the purposes of the present study. Thus, 176 peaks (88 different m/z in positive ionization mode and 88 in negative) were selected based on their specific distribution and intensity in the rat brain (Supplemental material S1). However, we were only able to assign 51 molecules to specific lipid species in positive ionization mode and 34 in negative. The lipid species were grouped into common lipid families to facilitate the interpretation of results.

Differences between CSF and SAP-treated rats were analyzed using Student's parametric t test followed by Bonferroni's post-hoc test with GraphPad Prism (San Diego, CA, USA). The results were considered significant when $p \leq 0.05$. A subsequent alignment was necessary because of a spectrometer de-calibration of 0.008 units.

3. Results and Discussion

The results are discussed here starting first with the class of lipid species that has been identified and localized in the rat brain. In the second part, the anatomical localization of lipid molecules is used to discuss the involvement of different lipid types in the overall lipid composition of each part or structure of the brain (brainstem, mesencephalon, cerebellum, diencephalon and telencephalon). The discussion also considers the physiological implications of those specific distributions.

3.1 Distribution of lipids by category

The different lipid species present in the rat brain were detected in positive ionization mode in the range of m/z= 500-1000, or in negative ionization mode in the range of m/z= 400-1100, depending on the ionization of the molecule in the presence of the MBT matrix. Scanning was performed in several different brain sections and from different animals. However, one representative section was selected to show the results for easier comparison. The distribution pattern of each of the selected lipid species in the same brain section was obtained. The results are displayed with the selected lipid species grouped into the two main categories of phospholipids and sphingolipids.

3.1.1. Phospholipids

Phospholipids are the primary components of the plasma membrane. Some of them can act as secondary messengers. These include phosphoinositides, which are derived from phosphoinositols. Phosphoinositols are in turn implicated in intracellular signaling cascades following the activation of specific phospholipases, such as PLC in mammalian cells [25]. The recorded intensities of the seven different sub-categories of phospholipids are described as follows: phosphatidylcholines, phosphatidylethanolamines, lysophospholipids, phosphatidylinositols, phosphatidic acids, phosphatydilglycerols and phosphatidylserines.

3.1.1.1. Phosphatidylcholines (PC)

PCs are one of the major components of the mammalian plasma membrane [26], are associated with a large number of cellular processes and are precursors of other lipids that possess simple chemical structure. These include the free fatty acids and

lysophospholipids formed by degradation of PC by phospholipase A_2 (PLA_2), which is responsible for hydrolyzing sn-2 ester bonds [27]. The PC (34:1) detected as PC (34:1) + H^+ (m/z = 760.5810) and PC (34:1) + K^+ (m/z = 798.5497), was found distributed throughout the rat brain, showing high intensities of 52.49% and 100%, respectively, that indicate its significant presence in the majority of all types of cell membranes. In contrast, other PC species such as PC (36:1) (detected as PC (36:1) + H^+ (m/z= 788.6157) or PC (36:1) + K^+ (m/z= 826.5719) was detected specifically in white matter. In gray matter, PC (32:0) + K^+ (m/z= 772.5296) was present at high intensities (75.81%) (Figure 1). This general distribution of PC species is in agreement with previously reported results from *postmortem* human brain [15]. Moreover, some PC species were only present in very discrete areas of the rat brain. These included PC (32:4) + K^+ (m/z= 764.4633), which was detected primarily in the choroid plexus (0.21%) (Figure 1). The physiological role of each PC species in specific brain cell types remains to be elucidated. However, the anatomical pattern of PC intensity distribution can be compared with that of the human brain for neurological and/or neuropathological studies.

3.1.1.2. Lysophospholipids

Some lysophospholipids are intercellular mediators that act as signaling molecules to specifically activate G protein-coupled receptors [17,28]. The lysophospholipid species detected here that have been already identified in the Lipid Maps database and, showed low densities in the rat CNS were: CPA (18:0) – H^+ (m/z= 419.2560) and LPA (18:0) – H^+ (m/z= 437.2658) (6.46% and 2.64% density, respectively). These two molecules exhibited a uniform distribution throughout the brain, suggesting their involvement in many physiologically important processes. LPA regulates neuronal plasticity [29], neurogenesis [2,3], myelination and cell migration [4-6].

Conversely, the lysophosphatidylcholine (LPC) (16:0) - CH_3^+ (m/z= 480.497) was detected at a higher relative intensity than LPC (18:0) - CH_3^+ (m/z= 508.3386), although the patterns of distribution were comparable (4.17% and 0.44%). These LPC species are up-regulated in neuropathological situations such as inflammatory processes [30]. Modulation of the distribution of LPC (16:0) and LPC (18:0) could be used as a marker of inflammation in specific areas of the brain.

The lysophosphatidylinositols (LPI) are known to bind to the GPR55 receptor [28] and may have a role in axonal growth [31]. Here, the LPI (18:0) – H^+ (m/z= 599.3215) presented a homogeneous distribution in gray matter areas (2.15%) (Figure 2, A).

3.1.1.3. Phosphatidylethanolamines (PE)

Together with PC, the PEs constitute the primary building blocks of the cell membrane. Consistent with this, the PE species that we were able to detect and assign to specific molecules, such as PE (18:0/18:1) – H^+ (m/z= 744.5537) and PE (P-18:0/22:6) – H^+ (m/z= 774.545), showed a homogeneous distribution in gray matter areas of the brain (1.25%). The relatively small size of PE's polar head confers on these molecules a conical form essential for curvature of membranes that is necessary for the fission and fusion processes, as well as to provide the proper fluidity to the membrane [32,33] (Figure 2, B). The conservation of the anatomical pattern of distribution may indicate the health of the above cell processes in animal models of disease.

3.1.1.4. Phosphatidic acids (PA)

PA species were also present in plasma membranes, but some could be uniquely localized to white matter areas of the brain where the presence of neuronal perikarya is scarce. These include PA (40:5) + H^+ (m/z= 751.5307) and PA (38:3) + K^+ (m/z= 765.4866) (2.86% and 2,31% density, respectively). Other PA species were detected in gray matter: PA (39:0) + Na^+ (m/z= 769.5683) and PA (O-40:1) / PA (P-40:0) + K^+ (m/z= 783.5685) (33.97% and 15.31%). PA can influence the curvature of the membrane and act as a lipid signal by recruiting cytosolic proteins to a specific position on the membrane [34-36]. Moreover, some PA species demonstrate a unique distribution that may correspond to areas with high levels of cell division (e.g., epithelial cells at the choroid plexus) and/or differentiation (e.g., neurogenesis in adults at the dentate gyrus of the hippocampus). In the current study, these included PA (O-31:0) + H^+ (m/z= 621.4848), PA (38:5) + K^+ (m/z= 761.4528) and PA (36:2) + K^+ (m/z= 739.4697) (0.53%, 3.89% and 35.21%) [37]. The latter can even be observed at the rostral migratory stream that is one of the few brain regions with periglomerular neural progenitors [38] (Figure 3).

3.1.1.5. Phosphatidylinositols (PI)

The PIs constitute a group of phospholipids that commonly act as intracellular secondary messengers and function in intercellular signaling (Waugh, 2015 [25]). Our results found some PI species with a preferential distribution in white matter: PI (O-30:1) / PI (P-30:0) + H^+ (m/z= 767.5074) (12.74%) and PI (39:0) – H^+ (m/z= 907.6303) (34.02%) (Figure 4). Other PI species, however, displayed their highest intensity in

gray matter PI (18:0/20:4) – H^+ (m/z= 885.5530) (100%) and PI (O-40:5) / PI (P-40:4) – H^+ (m/z= 897.5864) (5.57%). One possibility is that the PI species localized to gray matter could have a greater role in inter-neuronal signaling. PI species may also act as secondary messengers in glial cells. This process involves phosphorylation of the hydroxyl groups in positions 3, 4 and / or 5 by different kinases in different part of the biomembranes to generate seven structurally different phosphoinositides. These in turn selectively recruit proteins responsible for intracellular signaling in multiple processes in different organelles [39] (Figure 4).

3.1.1.6. Phosphatidylglicerols (PG)

The physiology of PG is still poorly understood. The PG species that were detected and assigned to specific molecules showed low intensity and were found mainly in white matter: PG (40:5) + H^+ (m/z= 825.5667) (3.65%) and PG (39:5) - H^+ (m/z= 809.5331) (2.74%). However, some PG, such as PG (32:1) + Na^+ (m/z= 743.4839) (0.89%), were located in the gray matter (Figure 5). Additional insight into this distribution and these intensities in the rat CNS would contribute to the understanding of the role of these molecules in the brain.

3.1.1.7. Phosphatidylserine (PS)

PS is known to be selectively present in the inner leaflet of the plasma membrane in healthy cells. Here, some PS species were detected with low intensity, such as PS (37:2) + H^+ (m/z= 802.5561) (3.18%) and PS (34:1) - H^+ (m/z= 760.5161) (1.08%), and displayed an even distribution along the gray matter (Figure 5). Externalization of PS to the outer leaflet occurs early in apoptosis, providing a signal to induce phagocytosis of the cell [40]. Modification of the described pattern of anatomical distribution in both rodent models of disease and human brain samples could be an indicator of apoptotic processes occurring in the CNS.

3.1.2. Sphingolipids

3.1.2.1. Sphingomyelins (SM)

SM species are essential modulators of the properties of the plasma membrane because they are able to participate in the formation of lipid rafts [41]. Here, some SM species were detected specifically in white matter, such as SM (d42:2) + H^+ (m/z=

813.6853) (0.67%) and SM (d41:2) – H^+ (m/z= 797.6522) (5.22%). However, other SM showed a preferential location to gray matter, such as SM (d18:1/18:0) - CH_3^+ (m/z= 715.5738) (44.17%) and SM (d36:1) + Na^+ (m/z= 753.5899) (8.86%). It is possible that the species located in gray matter could be controlling neuronal processes and, therefore, be implicated in neurotransmission in some way [42]. Conversely, some SM species were distributed only in the choroid plexus. These included SM (d18:2/21:0) - H^+ (m/z= 769.6272) (0.18%) and SM (d39:1) – H^+ (m/z= 771.6390) (0.49%). Although the SM (d18:1/16:0) – H^+ (m/z= 687.5444) (1.49%) signal was intense in the choroid plexus, it was also present in gray matter (Figure 6). The content of the SM species listed above is strictly regulated through synthesis by sphingomyelin synthase, and through degradation by sphingomyelinases. SM degradation results in ceramides, which are the central component of sphingolipid metabolism. Alterations in these metabolic processes of SM, as well as in sulfatides (ST) have been associated with neurodegenerative diseases including Alzheimer's disease (AD) [43]. The discovery of alterations in the reported pattern of distribution in animal models and patients is contributing to the identification of new therapeutic targets (see further results in section 3.3) (in this same BBA-Biomembranes issue) [44].

3.1.2.2. Sulfatides (ST)

STs are a major component in the CNS, where they constitute an important component of myelin. Consequently, we found ST species distributed in white matter. However, not all ST showed a uniform distribution in the axonal tracts that constitute the most myelinated areas of the brain. Notably, ST (d18:1/18:0) – H^+ (m/z= 806.5469) (39.99%) signal was intense in the anterior commissure, while ST (d18:1/22:0) – H^+ (m/z= 878.6024) (24.94%) and ST (d18:1/24:1) – H^+ (m/z= 822.5369) (10.00%) were present at high levels in the anterior part of the anterior commissure (Figure 7). Therefore, the modulation of ST may indicate alterations in myelination processes.

3.1.2.3. Glycosphingolipid (GSL)

Several species of GSL were detected and assigned to specific molecules. For example, glucosylceramides (GlcCer) as GlcCer (d30:1) + K^+ (m/z= 682.4606) (0.58%) and GlcCer (d38:1) + Na^+ (m/z= 778.6187) (0.14%) displayed a restricted distribution to the choroid plexus. That specific localization indicates a specialized role in epithelial cells. Moreover, the lactosylceramides (LacCer), such as LacCer (d30:1) + H^+ (m/z= 806.5578) (5.99%), were localized in the gray matter (Figure 8). Both species are precursors of complex GSLs such as gangliosides. These species are localized on the

surface of the plasma membrane and are synthesized from ceramide by the sequential addition of sugars by different glycosyltransferases [45].

3.2. Anatomical distribution of lipids in the brain

The mammalian brain can be divided into four large structures based on the functions that they control, their anatomical location and evolutionary terms. The brainstem (including midbrain or mesencephalon, medulla or myelencephalon and pons or metencephalon) constitutes the most archaic structure; the cerebellum; the diencephalon (thalamus and hypothalamus) and the telencephalon (including the cerebral cortex, basal ganglia and main parts of the limbic system). The following discussion about the relative intensity of signal in each area of the brain is based on observation of the color-coded images. The ratio of intensity of each molecule compared to the most abundant lipid species in the full section is mentioned above in section 3.1 and supplemental tables.

3.2.1. Brainstem

The results obtained in the rat brainstem showed that the most abundant lipids in this region are those found in white matter. Therefore, there is a relative abundance in the brainstem of different species of ST, specifically PC (36:1) + K^+ (Figure 1). The different nuclei and pathways located at the brainstem are primarily responsible for vegetative control, regulating vital life functions such as breathing and cardiac rhythm [46]. In addition, a large number of cranial nerves originate from this structure. Therefore, this area of the CNS is highly conserved across different animal species. The brainstem is composed mostly of white matter, although discrete gray matter nuclei of neurons are also present. However, the signal intensities obtained here from white matter make it difficult to detect the small nuclei composed of gray matter. Two possibilities exist to address this issue: increase the spatial resolution of the technique, or obtain the lipid profile of the different cell types present at the CNS (neurons, glial and epithelial cells), localizing the distribution of the most abundant cell types (mostly neurons) in the gray matter.

The mesencephalon constitutes the confluence of the brainstem with other regions of the brain. The most dorsal part of this structure is called the superior colliculus, which is related to vision. The inferior colliculus is involved more in auditory processes [47,48]. In this manner, the mesencephalon is also an area of information exchange, primarily composed of white matter tracts and fibers. The lipid profile observed here is

consistent with the rest of the brainstem, although some characteristic gray matter lipids can be found. The PC (40:6) + H^+ showed a specific localization in the inferior colliculus. This could indicate a relationship to the auditory system, as the same lipid is also found in the cerebellum, which controls equilibrium signals from the inner ear (Figure 1). Furthermore, PA species are also detected throughout the mesencephalon, as well as at relatively high intensities in other brain areas including the diencephalon, olfactory bulb and rostral migratory tract (Figure 3). This specific distribution may indicate that the PA species are related with the stimuli reception and neuronal sprouting [49].

3.2.2. Cerebellum

The cerebellum is assumed to be much younger than the brainstem in evolutionary terms. This area of the brain integrates sensory and motor pathways, and it is deeply interconnected with other parts of the brain, passing information received from the cerebral cortex to the locomotor system through motor pathways [50]. The most abundant lipid species in the white matter tracts of the cerebellum are ST and PC (36:1) + K^+, but there are other lipids that are only found in the telencephalon and diencephalon (Figures 1 and 7). Thus, PC (32:0) + K^+, PA (39:0) + Na^+ and SM (d18:1/18:0) - CH_3^+ are present at high levels in the molecular layer of the cerebellum, and PA (38:5) + K^+ and PC (38:7) + H^+, in the granular layer (Figures 1, 3 and 6). Further studies are necessary to connect these specific lipids to specialized functions of the cerebellum.

3.2.3. Diencephalon

The diencephalon is differentiated into two major structures: the thalamus, which is the main entrance for sensory stimuli (excluding olfactory signals), and the hypothalamus, which constitutes the control area for appetite, sleep and thirst and is involved in the processing of emotions [51]. The lipid composition of the diencephalon can also be distinguished by region. The lipids present in the thalamus are distributed homogeneously, but some parts of the hypothalamus show a different lipid composition. Some lipid species are evenly distributed in both thalamus and hypothalamus, including PC (32:0) + K^+, PA (36:2) + K^+, PI (18:0/20:4) - H^+ y PI (39:0) - H^+ (Figures 1, 3 and 4). In contrast, other lipid species are detected more intensely in the hypothalamus than in the thalamus. These include PA (39:0) + Na^+, SM (18:1/16:0) - H^+ y SM (d18:1/18:0) - CH_3^+ (Figures 3 and 6). The thalamus regulates sensory and

cognitive information being passed to the cortex, and alterations in the phospholipids PC, SM, and PS, as well as galactocerebrosides, have been reported in the thalamus of schizophrenic patients [52]. The results of this study in the rat CNS identify specific phospholipids in the thalamus that could be specifically altered in schizophrenia.

3.2.4. Telencephalon

The telencephalon is considered the most developed part of the brain, controlling and processing elaborated responses to stimuli. Several major structures can be distinguished, including the cerebral cortex, which is responsible for integration and interpretation of stimuli. The subcortical area of the telencephalon includes the hippocampus, which plays important roles in memory and spatial orientation. The basal ganglia that are localized adjacent to the hippocampus participate in the control of voluntary movements, and the olfactory bulbs, in the anterior part of the brain, process the information received from the olfactory system. Throughout the telencephalon, PA (39:0) + Na^+ is abundant, but with low intensity in the olfactory bulb (Figure 3). PC (32:0) + K^+, SM (d18:1/16:0) - H^+ and SM (d18:1/18:0) - CH_3^+ also displayed high intensities (Figures 1 and 6). Regarding the different sub-structures, it is remarkable to note the presence of ST species in the innermost layers of the cerebral cortex adjacent to the corpus callosum. The STs are abundant in white matter fibers, and layers V-VI of the cerebral cortex receive the input of a plethora of axons from the corpus callosum. Here, the presence of ST in oligodendrocytes could account for this relative abundance (Figure 6). In the olfactory bulb, it is important to note the presence of specific lipid species with a high intensity, e.g., PG (39:5) - H^+ and PC (34:3) + H^+, that are not present in other telencephalic structures such as the hippocampus, where PI-Cer (d18:0/16:0) + Na^+ is abundant in the granular layer of the dentate gyrus (Figure 1 and supplemental material). The physiological role of each of the described lipid species in each area should be further elucidated to understand their involvement in specific neurological diseases, as was recently described for multiple system atrophy [53].

3.3. Distribution of lipids in the rat model of cholinergic basal forebrain lesion

Animal models are essential to understand the pathological mechanisms underlying neurodegenerative diseases. To study new treatments for Alzheimer's disease, different transgenic mouse models have been developed to display neuropathological markers and carry familiar mutations. However, there are also rat models based on the specific cholinergic impairment of the basal forebrain. Different studies have been

conducted in which the cholinergic system was injured to produce similar memory and learning deficits as those observed in AD [54-56]. Therefore, the selective degeneration of cholinergic neurons provides the opportunity to study biochemical, neuroanatomical and behavioral aspects to those occurring in AD. In the present study, a specific antibody-driven toxin, 192IgG saporin (SAP), induced selective lesions in the rat basal forebrain to impair memory and learning processes in a manner similar to the clinical manifestations of AD. In order to check the involvement of the cholinergic neurons in the basal forebrain area in the impairment in learning and memory, a specific behavioral test for cholinergic system mediated learning was performed, the passive avoidance maze. The results showed that all the animals of the aCSF group achieved the established maximum time in the learning latency, but SAP group spent a mean of 40 ± 32 sec before entering to the dark compartment, indicating the effectiveness of the lesion. In addition, we counted the number of positive cholinergic neurons in the area where the toxin was injected, resulting in a dramatic decrease of cholinergic cells (aCSF: 888 ± 175; SAP: 124 ± 48 AChE cells/mm^3; $p<0.05$). Linear regression between the passive avoidance step-through latency times and the number of surviving cholinergic cells in the nucleus basalis magnocellularis (NMB) showed a positive correlation ($r = 0.71$; $p<0.005$) (Figure 9). The used rat model of cholinergic basal forebrain lesion, has been used before with controversial results regarding the impairment in learning and memory [57,58]. The basal forebrain area is located ventrally in the rat brain and the tract of the needle can produce a tissue damage that may be affecting to learning and memory, as we have previously observed (unpublished results). In this context, we have improved the surgical procedures by using an ultrathin gauge needle, which dramatically reduces the needle damage during the toxin administration. In addition, the behavioral test of passive avoidance was performed to validate the lesion model, evaluating the impairment in learning and memory. A positive correlation between the decrease of cholinergic neurons in the basal forebrain and the step-through latency times was obtained.

The IMS study of the lipid profile in the CNS of this animal model was compared to control rats receiving SAP versus the vehicle, aCSF. SAP administration produced a specific lesion in basal forebrain cholinergic cells, causing a subcortical cholinergic denervation [59]. Here, after death of the NBM cholinergic cells, some ST species were detected with less intensity in the NBM of rats with lesions: ST(d18:1/22:0) (aCSF: 23,18 ± 2,77% vs 192IgG-Sap: 13,13 ± 2,594%), ST(d18:1/24:1) (aCSF: 63,27 ± 5,078% vs 192IgG-Sap: 32,53 ± 7,375%), ST(d18:1/24:0) (aCSF: 38,39 ± 2,298% vs 192IgG-Sap: 19,92 ± 4,335%), ST(d18:1/h24:1) (aCSF: 45,35 ± 4,278% vs 192IgG-

Sap: 22,93 ± 5,049%), ST(d18:1/h24:0) (aCSF: 54,16 ± 4,191% vs 192IgG-Sap: 27,50 ± 5,981%). Conversely, other lipid species were significantly up-regulated in this same area, including LPC (18:0) – H^+ (aCSF: 0,41 ± 0,139% vs 192IgG-Sap: 0,84 ± 0,114%) (Figure 10).

Taking into account these results, changes in the lipid profile of NBM of SAP-treated rats could be similar to those occurring in the brain of AD patients. Certainly, one of the most consistent lipid changes that has been described in brains of AD patients is the decrease of sulfatides during the early stages of disease [18,60]. Cheng et al. have reported that this decrease can be related to neuronal loss in a manner similar to that in our rat model of AD, because in the SAP-injured area, sulfatides are decreased significantly due to the induced death of NBM cholinergic neurons. This finding validates the model for the assay of new treatments designed to restore lipid homeostasis. The specific vulnerability of cholinergic cells in AD could be related to the specific lipid alterations described.

Conversely, the increase of LPC observed in the injured area may be related to pro-inflammatory effects. The result of the degradation of cell membranes generates signaling intermediaries such as LPC [61].

4. Conclusions

Our results demonstrate that lipids may have specific distributions based on the lipid type and fatty acid component, giving rise to very specific locations in the rat brain related to the physiology of the cells controlling specific functions. Thus, certain of these lipids could also constitute a reservoir of specific molecules involved in cell signaling and neurotransmission when relevant enzymes activate secondary messengers, generating different specific lipid species on demand in each area of the brain. Moreover, altering specific lipids involved in the neuropathology of neurodegenerative diseases such as AD could be a good approach for providing new therapeutic strategies. For all of the above-mentioned reasons, lipids are becoming a family of biomolecules with increasing potential in the development of new therapies for neurodegenerative diseases.

Acknowledgements

Supported by grants from the regional Basque Government IT975-16 and ELKARTEK16/81 and Spanish Government, Ministry for Health, I. S. C. III PI 10/01202, partially financed by F.E.D.E.R.; European Union. Technical support

provided by the analytical unit SGIKER (UPV/EHU, MICINN, GV, ESF) is gratefully acknowledged. A. Ll.-O. is a recipient of a predoctoral fellowship from the Basque Government.

Figures

Figure 1. Representative IMS images corresponding to assigned lipids of the PC subclass. The distribution of the relative abundance of the recorded signal intensity is shown in color-coded individual images of each PC throughout a representative sagittal section of the rat brain. PC (34:1) + K^+ (m/z 798.5497) was the most abundant PC throughout the whole tissue but also the lipid detected with the highest average intensity when all pixels of the image were considered. PC (36:1) was found primarily in white matter, and PC (32:0) in gray matter. The PCs were detected in positive ionization using the same parameters in all sagittal sections of control rats: 100 µm spatial resolution, 10 shot per point at laser fluence of 40 µJ. The color-coded bar representing the intensity ratio of the most abundant species in positive mode (PC (34:1) + K^+) is included.

Figure 2. IMS images showing the pattern of distribution of the intensities recorded for lysophospholipid (A) and PE lipid species (B) in a sagittal section of the rat brain. (A) The different lysophospholipids were detected at a relatively low intensity in gray matter. (B) PE species were also distributed primarily in gray matter. Both lysophospholipids and PE species were detected in negative ionization, and the recorded intensities were calculated as a % of the most abundant lipid species detected in negative ionization mode (PI (18:0)/ (20:4) - H^+; m/z 885.55340), using the following parameters: 100 µm spatial resolution, 10 shot per point at laser fluence of 40 µJ.

Figure 3. Representative IMS images corresponding to the intensity map of distribution of PA lipid species in the rat brain. Note that some species of PA were specifically located at the choroid plexus, e.g., PA (38:5). PA (40:5) was distributed primarily in white matter. In contrast, PA (39:0) showed a very specific distribution with high intensities in some gray matter areas of the diencephalon and cerebellum, such as external layers of the cortex, hippocampus and basal ganglia. This group was detected in positive ionization mode, using the following parameters: 100 µm spatial resolution, 10 shot per point at laser fluence of 40 µJ.

Figure 4. IMS images of lipid species identified as PI in the rat CNS. (A) Two PI molecules were detected in positive ionization, and (B) four in negative ionization mode. Note the relatively high intensities of PI (39:0) - H+ in the brain stem, thalamus colliculus and myelinated fiber bundles throughout the rat brain.

Figure 5. IMS images showing the anatomical distribution of the intensity signals for different PG (A) and PS (B) lipid species in a sagittal section of the rat brain. PG and PS species were detected in both positive and negative ionization depending on the molecule. The recorded intensities for both PG and PS were low compared with those of other lipids.

Figure 6. IMS images of the intensities recorded for different types of SM in rat CNS. (A) In positive ionization mode some molecules such as SM (d36:1) showed a uniform distribution in gray matter. (B) In negative ionization mode SM (d18:1/18:0) was also detected in gray matter, but SM (d18:1/16:0) was detected in the choroid plexus and in the borders of the brain, most likely in ependymal cells.

Figure 7. IMS images showing the pattern of distribution of ST species in the rat brain. All of the ST species detected were distributed along the white matter areas of the brain with moderate to high intensity. This group was detected in negative ionization mode.

Figure 8. Representative IMS images of GSL. (A) The GclCers were found distributed specifically in the choroid plexus. (B) LacCer (d30:1) was present with an even distribution along the gray matter areas of the rat brain.

Figure 9. The plot shows the number of cholinergic neurons in the NBM ($AChE^{+}$ /mm^3) and the step through latency times recorded in the passive avoidance test from 192IgG-saporin (n = 10) treated rats. The linear regression analysis reveals that those animals with higher reductions in BFCN density showed significantly lower step through latency times.

Figure 10. Coronal IMS images of representative rats corresponding to the NBM lesion model induced by IgG192-Saporin (SAP) compared to the same anatomical level of the control animals treated with aCSF. Note that all the ST species detected showed a lower intensity in the lesion area, indicating the specificity of lesions to cholinergic neurons. Moreover, LPC (18:0) was detected with a higher intensity in the lesioned animals. All of these species were detected in negative ionization, using the following parameters: 150 µm spatial resolution, 10 shots per point at laser fluence of 15-20 µJ.

References

[1] M. Murakami, Lipid mediators in life science, Exp.Anim. 60 (1) (2011) 7-20.

[2] J.H. Hecht, J.A. Weiner, S.R. Post, J. Chun, Ventricular zone gene-1 (vzg-1) encodes a lysophosphatidic acid receptor expressed in neurogenic regions of the developing cerebral cortex, J.Cell Biol. 135 (4) (1996) 1071-1083.

[3] Y.C. Yung, T. Mutoh, M.E. Lin, K. Noguchi, R.R. Rivera, J.W. Choi, M.A. Kingsbury, J. Chun, Lysophosphatidic acid signaling may initiate fetal hydrocephalus, Sci.Transl.Med. 3 (99) (2011) 99ra87.

[4] J.A. Weiner, J.H. Hecht, J. Chun, Lysophosphatidic acid receptor gene vzg-1/lpA1/edg-2 is expressed by mature oligodendrocytes during myelination in the postnatal murine brain, J.Comp.Neurol. 398 (4) (1998) 587-598.

[5] N. Fukushima, S. Shano, R. Moriyama, J. Chun, Lysophosphatidic acid stimulates neuronal differentiation of cortical neuroblasts through the LPA1-G(i/o) pathway, Neurochem.Int. 50 (2) (2007) 302-307.

[6] B. Anliker, J.W. Choi, M.E. Lin, S.E. Gardell, R.R. Rivera, G. Kennedy, J. Chun, Lysophosphatidic acid (LPA) and its receptor, LPA1 , influence embryonic schwann cell migration, myelination, and cell-to-axon segregation, Glia 61 (12) (2013) 2009-2022.

[7] A. Olivera, S. Spiegel, Sphingosine-1-phosphate as second messenger in cell proliferation induced by PDGF and FCS mitogens, Nature 365 (6446) (1993) 557-560.

[8] J. Alfonso, H. Penkert, C. Duman, A. Zuccotti, H. Monyer, Downregulation of Sphingosine 1-Phosphate Receptor 1 Promotes the Switch from Tangential to Radial Migration in the OB, J.Neurosci. 35 (40) (2015) 13659-13672.

[9] O. Cuvillier, G. Pirianov, B. Kleuser, P.G. Vanek, O.A. Coso, S. Gutkind, S. Spiegel, Suppression of ceramide-mediated programmed cell death by sphingosine-1-phosphate, Nature 381 (6585) (1996) 800-803.

[10] A. Olivera, H.M. Rosenfeldt, M. Bektas, F. Wang, I. Ishii, J. Chun, S. Milstien, S. Spiegel, Sphingosine kinase type 1 induces G12/13-mediated stress fiber formation, yet promotes growth and survival independent of G protein-coupled receptors, J.Biol.Chem. 278 (47) (2003) 46452-46460.

[11] D. Meyer zu Heringdorf, K. Liliom, M. Schaefer, K. Danneberg, J.H. Jaggar, G. Tigyi, K.H. Jakobs, Photolysis of intracellular caged sphingosine-1-phosphate causes Ca2+ mobilization independently of G-protein-coupled receptors, FEBS Lett. 554 (3) (2003) 443-449.

[12] M. Shen, S.A. Thayer, Cannabinoid receptor agonists protect cultured rat hippocampal neurons from excitotoxicity, Mol.Pharmacol. 54 (3) (1998) 459-462.

[13] C. Vazquez, R.M. Tolon, M.R. Pazos, M. Moreno, E.C. Koester, B.F. Cravatt, C.J. Hillard, J. Romero, Endocannabinoids regulate the activity of astrocytic hemichannels and the microglial response against an injury: In vivo studies, Neurobiol.Dis. 79 (2015) 41-50.

[14] L. Scalvini, D. Piomelli, M. Mor, Monoglyceride lipase: Structure and inhibitors, Chem.Phys.Lipids 197 (2016) 13-24.

[15] A. Veloso, R. Fernandez, E. Astigarraga, G. Barreda-Gomez, I. Manuel, M.T. Giralt, I. Ferrer, B. Ochoa, R. Rodriguez-Puertas, J.A. Fernandez, Distribution of lipids in human brain, Anal.Bioanal.Chem. 401 (1) (2011) 89-101.

[16] I. Manuel, G. Barreda-Gomez, E. Gonzalez de San Roman, A. Veloso, J.A. Fernandez, M.T. Giralt, R. Rodriguez-Puertas, Neurotransmitter receptor localization: from autoradiography to imaging mass spectrometry, ACS Chem.Neurosci. 6 (3) (2015) 362-373.

[17] E. Gonzalez de San Roman, I. Manuel, M.T. Giralt, J. Chun, G. Estivill-Torrus, F. Rodriguez de Fonseca, L.J. Santin, I. Ferrer, R. Rodriguez-Puertas, Anatomical location of LPA1 activation and LPA phospholipid precursors in rodent and human brain, J.Neurochem. 134 (3) (2015) 471-485.

[18] X. Han, D. M Holtzman, D.W. McKeel Jr, J. Kelley, J.C. Morris, Substantial sulfatide deficiency and ceramide elevation in very early Alzheimer's disease: potential role in disease pathogenesis, J.Neurochem. 82 (4) (2002) 809-818.

[19] M. Mapstone, A.K. Cheema, M.S. Fiandaca, X. Zhong, T.R. Mhyre, L.H. MacArthur, W.J. Hall, S.G. Fisher, D.R. Peterson, J.M. Haley, M.D. Nazar, S.A. Rich, D.J. Berlau, C.B. Peltz, M.T. Tan, C.H. Kawas, H.J. Federoff, Plasma phospholipids identify antecedent memory impairment in older adults, Nat.Med. 20 (4) (2014) 415-418.

[20] P. Davies, A.J. Maloney, Selective loss of central cholinergic neurons in Alzheimer's disease, Lancet 2 (8000) (1976) 1403.

[21] P.J. Whitehouse, D.L. Price, R.G. Struble, A.W. Clark, J.T. Coyle, M.R. Delon, Alzheimer's disease and senile dementia: loss of neurons in the basal forebrain, Science 215 (4537) (1982) 1237-1239.

[22] R.T. Bartus, R.L. Dean 3rd, B. Beer, A.S. Lippa, The cholinergic hypothesis of geriatric memory dysfunction, Science 217 (4558) (1982) 408-414.

[23] G. Paxinos, C. Watson, The Rat Brain in Stereotaxic Coordinates, 5th Edn (2005) San Diego, Elsevier Academic Press.

[24] G. Robichaud, K.P. Garrard, J.A. Barry, D.C. Muddiman, MSiReader: an open-source interface to view and analyze high resolving power MS imaging files on Matlab platform, J.Am.Soc.Mass Spectrom. 24 (5) (2013) 718-721.

[25] M.G. Waugh, PIPs in neurological diseases, Biochim.Biophys.Acta 1851 (8) (2015) 1066-1082.

[26] J.S. O'Brien, E.L. Sampson, Lipid composition of the normal human brain: gray matter, white matter, and myelin, J.Lipid Res. 6 (4) (1965) 537-544.

[27] B.S. Cummings, J. McHowat, R.G. Schnellmann, Phospholipase A(2)s in cell injury and death, J.Pharmacol.Exp.Ther. 294 (3) (2000) 793-799.

[28] S. Oka, K. Nakajima, A. Yamashita, S. Kishimoto, T. Sugiura, Identification of GPR55 as a lysophosphatidylinositol receptor, Biochem.Biophys.Res.Commun. 362 (4) (2007) 928-934.

[29] V. Garcia-Morales, F. Montero, D. Gonzalez-Forero, G. Rodriguez-Bey, L. Gomez-Perez, M.J. Medialdea-Wandossell, G. Dominguez-Vias, J.M. Garcia-Verdugo, B. Moreno-Lopez, Membrane-derived phospholipids control synaptic neurotransmission and plasticity, PLoS Biol. 13 (5) (2015) e1002153.

[30] C. Stock, T. Schilling, A. Schwab, C. Eder, Lysophosphatidylcholine stimulates IL-1beta release from microglia via a P2X7 receptor-independent mechanism, J.Immunol. 177 (12) (2006) 8560-8568.

[31] H. Cherif, A. Argaw, B. Cecyre, A. Bouchard, J. Gagnon, P. Javadi, S. Desgent, K. Mackie, J.F. Bouchard, Role of GPR55 during Axon Growth and Target Innervation, Eneuro 2 (5) (2015) 10.1523/ENEURO.0011-15.2015. eCollection 2015 Sep-Oct.

[32] D. Marsh, Lateral pressure profile, spontaneous curvature frustration, and the incorporation and conformation of proteins in membranes, Biophys.J. 93 (11) (2007) 3884-3899.

[33] R. Dawaliby, C. Trubbia, C. Delporte, C. Noyon, J.M. Ruysschaert, P. Van Antwerpen, C. Govaerts, Phosphatidylethanolamine Is a Key Regulator of Membrane Fluidity in Eukaryotic Cells, J.Biol.Chem. 291 (7) (2016) 3658-3667.

[34] M.R. Ammar, N. Kassas, M.F. Bader, N. Vitale, Phosphatidic acid in neuronal development: a node for membrane and cytoskeleton rearrangements, Biochimie 107 Pt A (2014) 51-57.

[35] E.E. Kooijman, V. Chupin, N.L. Fuller, M.M. Kozlov, B. de Kruijff, K.N. Burger, P.R. Rand, Spontaneous curvature of phosphatidic acid and lysophosphatidic acid, Biochemistry 44 (6) (2005) 2097-2102.

[36] K.M. Henkels, T.E. Miller, R. Ganesan, B.A. Wilkins, K. Fite, J. Gomez-Cambronero, A Phosphatidic Acid (PA) conveyor system of continuous intracellular transport from cell membrane to nucleus maintains EGF receptor homeostasis, Oncotarget (2016).

[37] M.F. Paredes, S.F. Sorrells, J.M. Garcia-Verdugo, A. Alvarez-Buylla, Brain size and limits to adult neurogenesis, J.Comp.Neurol. 524 (3) (2016) 646-664.

[38] J.G. Mendoza-Torreblanca, E. Martinez-Martinez, M. Tapia-Rodriguez, R. Ramirez-Hernandez, G. Gutierrez-Ospina, The rostral migratory stream is a neurogenic niche that predominantly engenders periglomerular cells: in vivo evidence in the adult rat brain, Neurosci.Res. 60 (3) (2008) 289-299.

[39] T. Balla, Phosphoinositides: tiny lipids with giant impact on cell regulation, Physiol.Rev. 93 (3) (2013) 1019-1137.

[40] M.O. Li, M.R. Sarkisian, W.Z. Mehal, P. Rakic, R.A. Flavell, Phosphatidylserine receptor is required for clearance of apoptotic cells, Science 302 (5650) (2003) 1560-1563.

[41] P. Pathak, E. London, The Effect of Membrane Lipid Composition on the Formation of Lipid Ultrananodomains, Biophys J. 109 (8) (2015) 1630-1638.

[42] M.D. Ledesma, B. Brugger, C. Bunning, F.T. Wieland, C.G. Dotti, Maturation of the axonal plasma membrane requires upregulation of sphingomyelin synthesis and formation of protein-lipid complexes, Embo J. 18 (1999) 1761-1771.

[43] T.A. Couttas, N. Kain, A.K. Suchowerska, L.E. Quek, N. Turner, T. Fath, B. Garner, A.S. Don, Loss of ceramide synthase 2 activity, necessary for myelin biosynthesis, precedes tau pathology in the cortical pathogenesis of Alzheimer's disease, Neurobiol.Aging 43 (2016) 89-100.

[44] E. González de San Román, I. Manuel, M.T. Giralt, I. Ferrer, R. Rodríguez-Puertas. Imaging mass spectrometry (IMS) of cortical lipids from preclinical to severe stages of Alzheimer's disease, BBA Biomembranes (2017).

[45] S. Basu, B. Kaufman, S. Roseman, Enzymatic synthesis of ceramide-glucose and ceramide-lactose by glycosyltransferases from embryonic chicken brain, J.Biol.Chem. 243 (1968) 5802-5804.

[46] J.C. Smith, H.H. Ellenberger, K. Ballanyi, D.W. Richter, J.L. Feldman, Pre-Botzinger complex: a brainstem region that may generate respiratory rhythm in mammals, Science 254 (5032) (1991) 726-729.

[47] U.C. Drager, D.H. Hubel, Responses to visual stimulation and relationship between visual, auditory, and somatosensory inputs in mouse superior colliculus, J.Neurophysiol. 38 (3) (1975) 690-713

[48] J.A. Winer, C.C. Lee, The distributed auditory cortex, Hear.Res. 229 (1-2) (2007) 3-13

[49] Y.B. Zhu, W. Gao, Y. Zhang, F. Jia, H.L. Zhang, Y.Z. Liu, X.F. Sun, Y. Yin, D.M. Yin, Astrocyte-derived phosphatidic acid promotes dendritic branching, Sci.Rep. 6 (2016) 21096.

[50] R. Apps, M. Garwicz, Anatomical and physiological foundations of cerebellar information processing, Nat.Rev.Neurosci. 6 (4) (2005) 297-311.

[51] T.V. Sewards, M.A. Sewards, Representations of motivational drives in mesial cortex, medial thalamus, hypothalamus and midbrain, Brain Res. Bull. 61(1) (2003) 25-49.

[52] A. Schmitt, K. Wilczek, K. Blennow, A. Maras, A. Jatzko, G. Petroianu, D.F. Braus, W.F. Gattaz, Altered thalamic membrane phospholipids in schizophrenia: a postmortem study, Biol.Psychiatry. 56 (5032) (2004) 41-45.

[53] A.S. Don , J.H. Hsiao , J.M. Bleasel , T.A. Couttas , G.M. Halliday , W.S. Kim, Altered lipid levels provide evidence for myelin dysfunction in multiple system atrophy, Acta Neuropathol Commun. 2 (2014) 150.

[54] F.A. Abdulla, M. Calaminici, J.A. Gray, J.D. Sinden, J.D. Stephenson, Changes in the sensitivity of frontal cortical neurones to acetylcholine after unilateral lesion of the nucleus basalis with alpha-amino-3-OH-4-isoxozole propionic acid (AMPA): effects of basal forebrain transplants into neocortex, Brain Res.Bull. 42 (3) (1997) 169-186.

[55] J. Berger-Sweeney, N.A. Stearns, S.L. Murg, L.R. Floerke-Nashner, D.A. Lappi, M.G. Baxter, Selective immunolesions of cholinergic neurons in mice: effects on neuroanatomy, neurochemistry, and behavior, J.Neurosci. 21 (20) (2001) 8164-8173.

[56] N.F. Fitz, R.B. Gibbs, D.A. Johnson, Selective lesion of septal cholinergic neurons in rats impairs acquisition of a delayed matching to position T-maze task by delaying the shift from a response to a place strategy, Brain Res.Bull. 77 (6) (2008) 356-360.

[57] M.G. Baxter, D.J. Bucci, L.K. Gorman, R.G. Wiley, M. Gallagher, Selective immunotoxic lesions of basal forebrain cholinergic cells: effects on learning and memory in rats, Behav.Neurosci. 109 (1995) 714-722.

[58] S. Rossner, Cholinergic immunolesions by 192IgG-saporin--useful tool to simulate pathogenic aspects of Alzheimer's disease, Int.J.Dev.Neurosci. 15 (1997) 835-850.

[59] E.M. Torres, T.A. Perry, A. Blockland, L.S. Wilkinson, R.G. Wiley, D.A. Lappi, S.B. Dunnet, Behavioural, histochemical and biochemical consequences of selective immunolesions in discrete regions of the basal forebrain cholinergic system, Neuroscience 63 (1) (1994) 95-122.

[60] H. Cheng, M. Wang, J.L. Li, N.J. Cairns, X. Han, Specific changes of sulfatide levels in individuals with pre-clinical Alzheimer's disease: an early event in disease pathogenesis, J.Neurochem. 127 (6) (2013) 733-738.

[61] J.K. Blusztajn, M. Liscovitch, U.I. Richardson, Synthesis of acetylcholine from choline derived from phosphatidylcholine in a human neuronal cell line, Proc. Natl. Acad. Sci. U. S. A. 84(15) (1987) 5474-7.

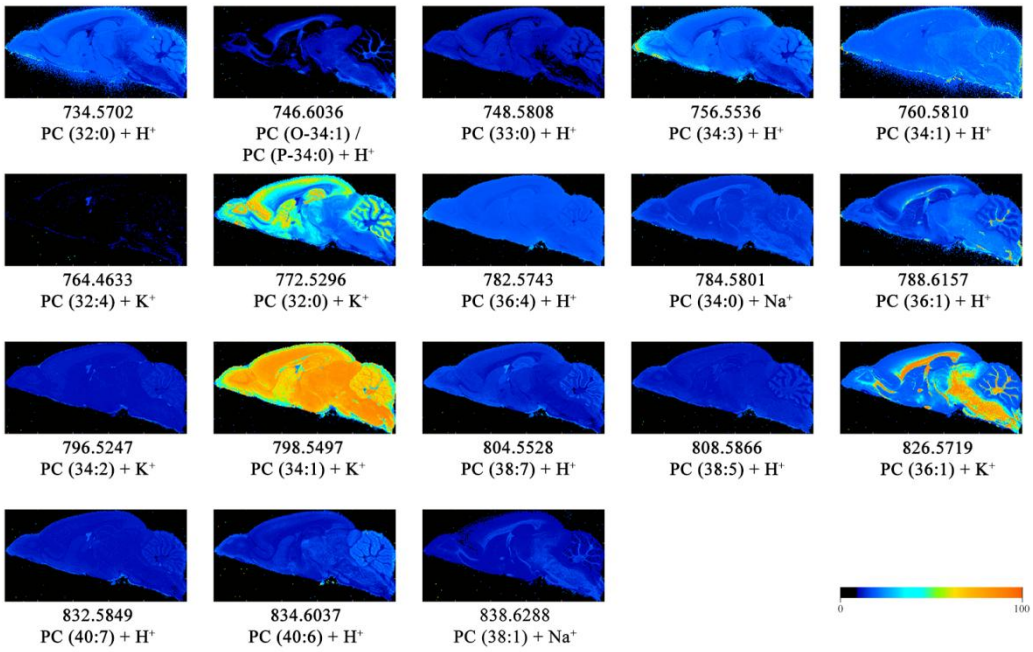

Figure 1

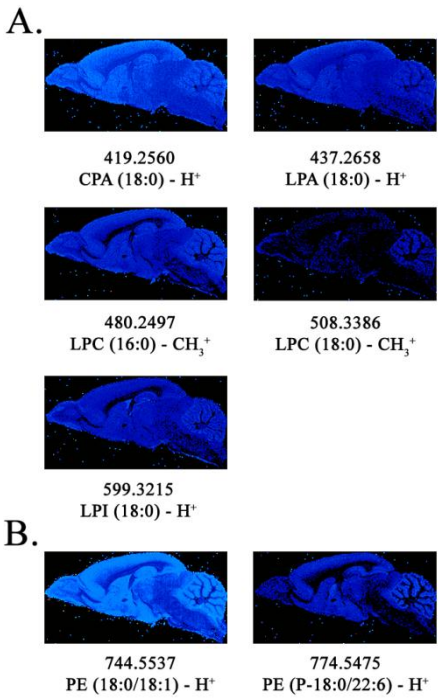

Figure 2

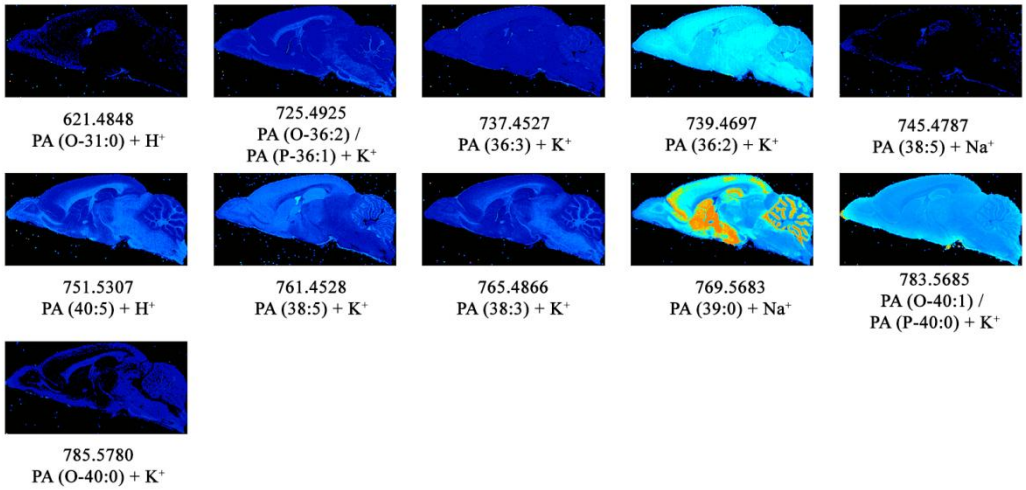

Figure 3

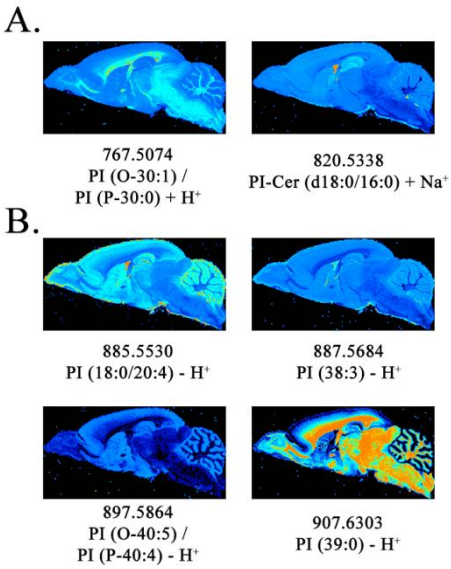

Figure 4

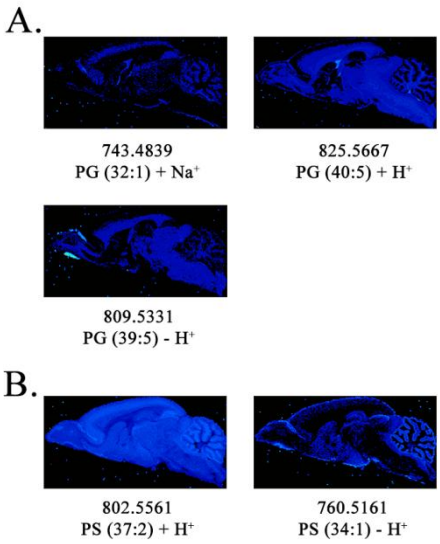

Figure 5

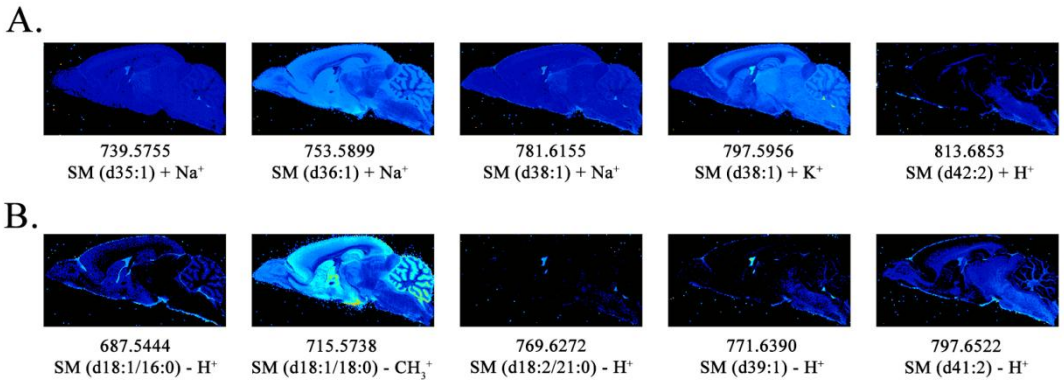

Figure 6

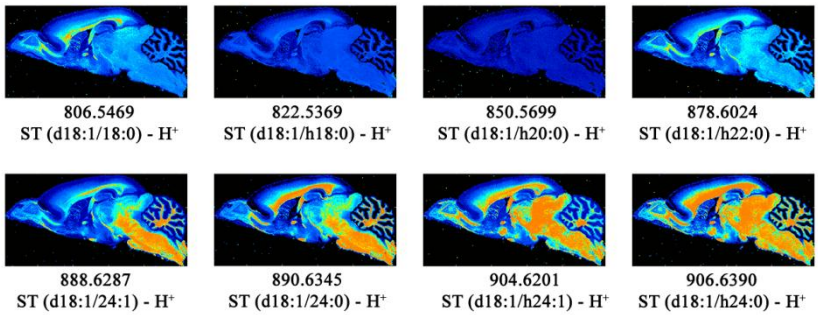

Figure 7

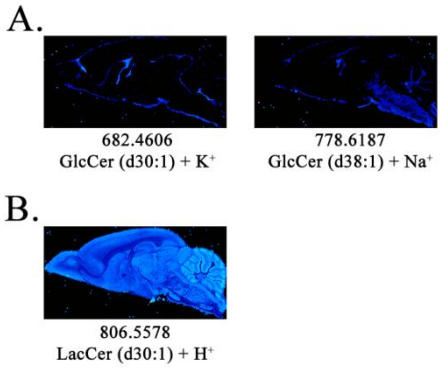

Figure 8

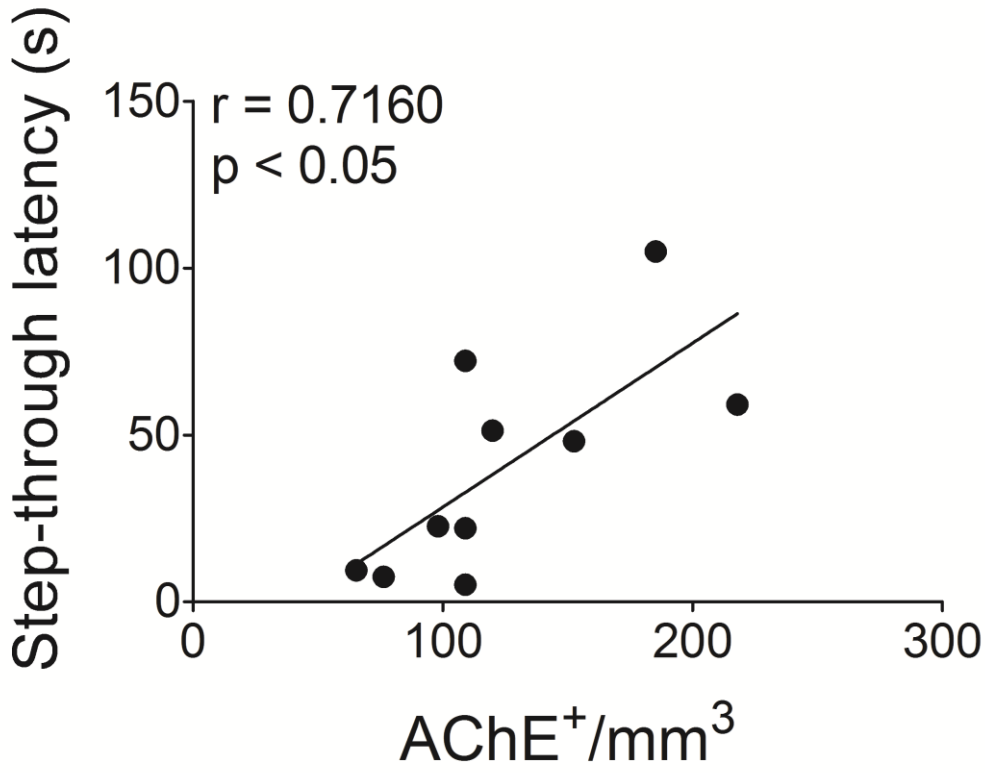

Figure 9

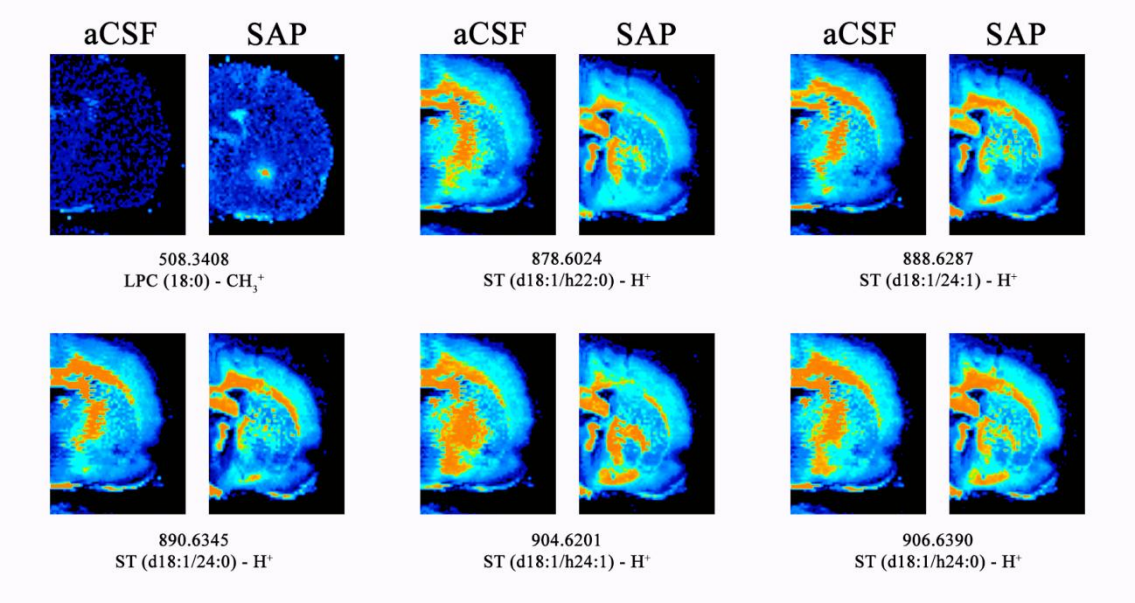

Figure 10

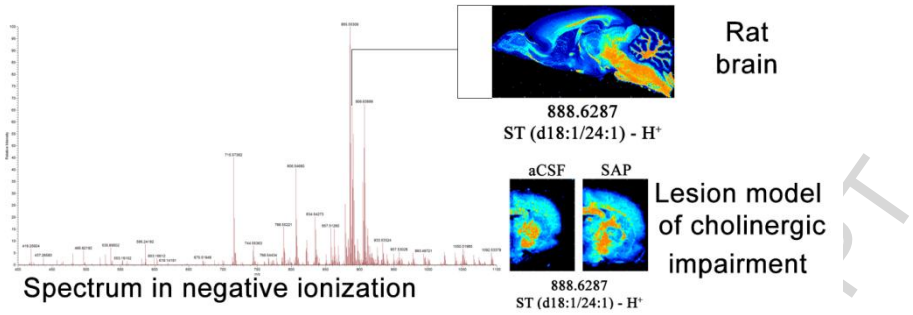

Graphical abstract

HIGHLIGHTS

- Distribution pattern of lipids families in rat CNS.
- Specific anatomical location of different lipids in rat CNS by IMS.
- Specific decrease of ST in lesion model of memory impairment.
- Applicability of MALDI-IMS for lipidomic studies in animal models of disease.